Magnetic Coupling in the Ce(III) Dimer $Ce_2(COT)_3$

Frédéric Gendron[a b], Jochen Autschbach[a], Jean-Paul Malrieu[c], Hélène Bolvin[c d *]

Contents

[a]Department of Chemistry, University at Buffalo, State University of New York, Buffalo, New York 14260-3000, United States

[b]Present address: Institut des Sciences Chimiques de Rennes UMR 6226 Université de Rennes 1 Campus de Beaulieu 35042 Rennes, France

[c]Laboratoire de Chimie et Physique Quantiques, CNRS, Université Toulouse III, 118 route de Narbonne, 31062 Toulouse, France

[d]On research leave at Hylleraas Center for Quantum Molecular Sciences, Department of Chemistry, University of Oslo, Norway for the period August 2017 to June 2018.

*e-mail address: bolvin@irsamc.ups-tlse.fr

S1 WFT results for $[Ce(COT)_2]^-$

Table S1: Energies (cm^{-1}) of the excited states calculated without (SF) and with SOC (SO) and g factors of the ground state for $[Ce(COT)_2]^-$ for the structures given in Table 1.

structure		CASPT2		B3LYP		X-rays	cryst sym [a]				+2 THF [b]
		CAS [c] SCF	CAS PT2	CAS SCF	CAS PT2	CAS SCF	CAS SCF	CAS PT2	RAS [d] SCF	RAS PT2	CAS SCF
SF	E_π	491	520	527	272	494-509	501	417	446	444	487-499
	E_ϕ	760	1079	630	1028	734	729	945	549	555	716
	E_δ	2347	2751	1962	2302	2188-2238	2213	2489	1951	2353	2170-2229
SO	$E_{5/2}$	646	957	488	1003	610	610.	872.	472	496	597
	$E_{3/2}$	1186	1308	1059	1136	1146	1146.	1229.	1080	1237	1140
	$E_{1/2'}$	2315	2317	2334	2328	2322	2322.	2317	2683	2683	2321
	$E_{7/2'}$	2839	3145	2712	3233	2815	2816	3071	3014	3015	2802
	$g_\parallel$	1.06	1.07	1.08	0.97	1.06	1.06	1.03	1.02	1.02	1.06
	$g_\perp$	-2.35	-2.34	-2.35	-2.46	-2.33	-2.35	-2.39	-2.44	-2.42	-2.34

a: symmetrized crystallographic structure according to $\mathcal{D}_{8h}$. *b*: crystallographic structure including the two closest THF molecules. *c*: CAS=CAS(1,7). *d*: RAS=RAS(9/7/4)

S2 DFT results for $[Ce_2(COT)_3]$

Table S2: $\left\langle \hat{S}^2 \right\rangle$ for triplet and BS states calculated with SR DFT for $[Ce_2(COT)_3]$ for the structures given in Table 1.

structure	B3LYP		PBE0		PBE	
	$\left\langle \hat{S}^2 \right\rangle_T$	$\left\langle \hat{S}^2 \right\rangle_{BS}$	$\left\langle \hat{S}^2 \right\rangle_T$	$\left\langle \hat{S}^2 \right\rangle_{BS}$	$\left\langle \hat{S}^2 \right\rangle_T$	$\left\langle \hat{S}^2 \right\rangle_{BS}$
DFT	2.00488	1.00473	2.00395	1.00385	2.01156	1.00369
PT2	2.00377	1.00254	2.00317	1.00226	2.00842	0.98175
EXAFS	2.00412	1.00114	2.00343	1.00099	2.00966	0.94978

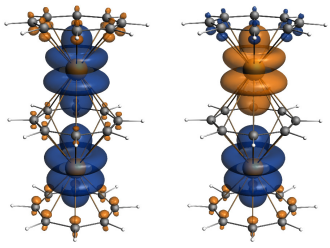

Figure S1: Isosurfaces (± 0.0005 au.) of SR DFT spin densities calculated for the spin triplet and BS states with the DFT structure.

S3 WFT results for $[Ce_2(COT)_3]$

Table S3: Energies (cm^{-1}) of the excited states of $[Ce_2(COT)_3]$ calculated with CI methods for the structures of Table 1. States arising from a same configuration are grouped, the degeneracy of which is given in parenthesis. Configurations are given according to orbitals and spinors defined in Scheme 1.

structure		EXAFS				PT2				DFT			
	conf	CASCI	CAS+S CI	DDCI2	DDCI3	CASCI	CAS+S CI	DDCI2	DDCI3	CASCI	CAS+S CI	DDCI2	DDCI3
SF	$f_\sigma f_\sigma$(2)	5.5	12.4	12.6	29.9	2.5	6.3	6.5	15.3	0.5	2.2	2.3	5.2
	$f_\sigma f_\pi$ (8)	679±2	617±2	618±2	840±6	635±2	572±2	548±2	752±3	618±1	560±1	5061±1	1065
	$f_\sigma f_\phi$ (8)	857±1	783±7	790±7		812±1	726±3	732±3		719±1	648±1	654±1	
	$f_\pi f_\pi$ (8)	1358±3	1232±5	1233±5	1676±5	1271±2	1142±4	1094±4	1501±4	1242±3	1128±4	1128±4	1422±5
	$f_\pi f_\phi$ (16)	1396±1	1375±4	1388±4		1305±1	1257±1	1268±1		1194±7	1152±7	1162±7	
	$f_\phi f_\phi$ (8)	1755±1	1581±4	1594±4		1658±1	1460±3	1472±3		1470±5	1308±6	1319±6	
	$f_\sigma f_\delta$ (8)	2154±23	2202±73	2225±74		2052±20	2077±50	2097±50		1736±7	1746±30	1763±35	
	$f_\pi f_\delta$ (16)	2688±17	2793±38	2820±38		2542±15	2607±35	2631±35		2207±10	2248±26	2268±28	
	$f_\delta f_\phi$ (16)	3034±19	3001±55	3028±55		2882±17	2813±47	2838±47		2474±10	2406±30	2428±33	
	$f_\delta f_\delta$ (8)	4320±35	4416±93	4459±94		4114±30	4164±90	4202±90		3483±19	3502±60	3534±67	
SO	$\frac{1}{2} \otimes \frac{1}{2}$ (4)	0.00	0.00	0.00	0.00	0.00	0.00	0.00	0.00	0.00	0.00	0.00	0.00
		2.80	6.36	6.46	15.50	1.83	3.15	3.46	8.15	0.00	0.29	0.27	2.20
		3.02	6.46	6.49	16.03	2.06	4.22	3.64	8.41	0.42	1.08	1.03	2.20
	$\frac{1}{2} \otimes \frac{5}{2}$ (8)	581±1	593±5	602±5	419±5	551±1	546±3	576±3	400±3	446±1	446±2	454±3	325±2
	$\frac{1}{2} \otimes \frac{3}{2}$ (8)	1130±5	1169±14	1167±13	1170±15	1083±6	1097±4	1110±10	1005±10	939±3	959±6	967±7	947±7
	$\frac{5}{2} \otimes \frac{5}{2}$ (4)	1324±1	1222±8	1236±6	1051±6	1260±1	1135±2	1171±4	995±5	1156±2	958±4	970±5	842±4
	$\frac{5}{2} \otimes \frac{3}{2}$ (8)	1720±3	1758±11	1774±10	1590±10	1642±3	1651±5	1689±6	1513±5	1412±5	1417±10	1432±10	1304±10
	$\frac{3}{2} \otimes \frac{3}{2}$ (4)	2243±5	2320±12	2337±5	2336±15	2147±4	2199±10	2217±9	2184±5	1869±4	1914±15	1930±15	1880±15
	$\frac{1}{2} \otimes \frac{1'}{2}$ (8)	2239±2	2330±5	2328±6	2375±5	2332±1	2336±2	2324±3	2354±4	2342±2	2337±2	2337±2	2357±3
	$\frac{1}{2} \otimes \frac{7}{2}$ (8)	2793±1	2798±3	2807±4	2624±4	2765±1	2753±2	2783±2	2608±2	2690±1	2683±1	2691±1	2563±1
	$\frac{5}{2} \otimes \frac{1'}{2}$ (8)	3901±1	2918±3	2928±4	2745±3	2868±1	2865±2	2898±3	2721±2	2777±1	2778±2	2843±1	2659±1
	$\frac{3}{2} \otimes \frac{1'}{2}$ (8)	3288±5	3360±18	3371±15	3301±10	3228±2	3273±7	3200±10	3235±7	3066±2	3097±6	3108±7	3072±7
	$\frac{1'}{2} \otimes \frac{3'}{2}$ (8)	3468±2	3480±9	3493±9	3530±15	3414±2	3421±5	3431±6	3452±10	3281±1	3293±4	3304±4	3300±7
	$\frac{5}{2} \otimes \frac{7}{2}$ (8)	3536±1	3428±5	3440±6	3255±5	3476±1	3343±3	3377±3	3101±2	3302±4	3198±4	3209±4	3080±4

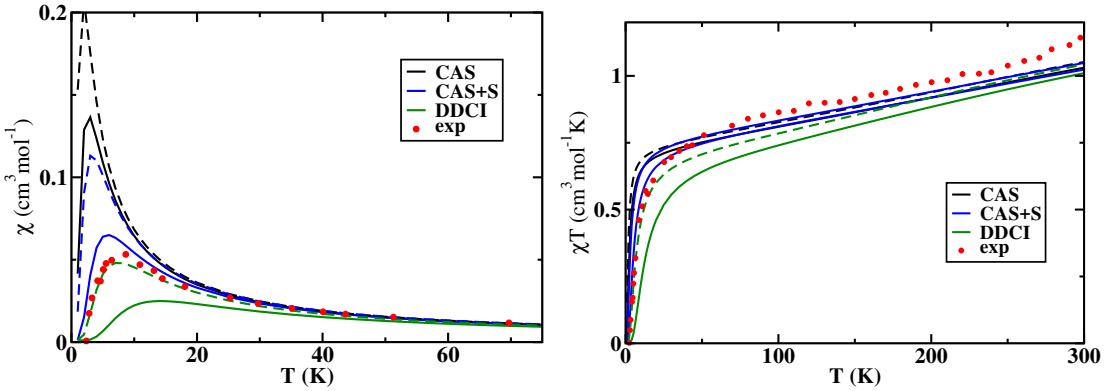

Figure S2: Susceptibility (left) and χT (right) vs T for $[Ce_2(COT)_3]$, experimental from [1] and calculated with CI methods, for *EXAFS* (full line) and *CASPT2* (dashed line) structures. DDCI2 curves are omitted since they superpose with CAS+S ones.

S4 Modelization of $[Ce(COT)_2]^-$ and $[Ce_2(COT)_3]$

S4.1 Model Hamiltonian for the monomer

In the pseudo-axial symmetry $\mathcal{D}_{8h}$, the ligand field splits the ground term $^5F_{5/2}$ of the free Ce(III) ion according to the value of $|M_J|$.[2] In the present case, the ground doublet is $|M_J| = 1/2$. The modelization is similar to $[U(\eta^7\text{-}C_7H_7)_2]^-$ as developed by Gourier *et al.*[3] and using the lines of the octahedral $5f^1$ AcX_6 series.[4] As in these two former examples, the g factors are determined by the 'competition' between CF and SO coupling. In the free ion, the spinors of the $|M_J| = 1/2$ KD are (using a $|J; M_J>$ notation)

$$\begin{aligned}
|\frac{5}{2};\frac{1}{2}> &= -\frac{\sqrt{3}}{\sqrt{7}}f_0 + \frac{2}{\sqrt{7}}\bar{f}_1 \\
|\frac{5}{2};-\frac{1}{2}> &= -\frac{\sqrt{3}}{\sqrt{7}}\bar{f}_0 + \frac{2}{\sqrt{7}}f_{-1} \\
|\frac{7}{2};\frac{1}{2}> &= \frac{2}{\sqrt{7}}f_0 + \frac{\sqrt{3}}{\sqrt{7}}\bar{f}_1 \\
|\frac{7}{2};-\frac{1}{2}> &= \frac{2}{\sqrt{7}}\bar{f}_0 + \frac{\sqrt{3}}{\sqrt{7}}f_{-1}
\end{aligned} \tag{S1}$$

where f_m and $\bar{f}_m$ are the spin-orbitals $R_{4f}(r)Y_{3m}(\theta,\phi)\alpha$ and $R_{4f}(r)Y_{3m}(\theta,\phi)\beta$ respectively, with spherical harmonics $Y_{lm}(\theta,\phi)$. z is the C_8 axis. These functions only imply σ and π orbitals with $|M_L| = 0$ and 1 respectively. We may restrict the model orbitals to those spin-orbitals and we introduce the notations

$$\begin{aligned}
\sigma_{1/2} &= f_0 = f_\sigma \\
\sigma_{-1/2} &= \bar{f}_0 = \bar{f}_\sigma \\
\pi_{1/2} &= \bar{f}_1 = \bar{f}_{\pi+} \\
\pi_{-1/2} &= f_{-1} = f_{\pi-}
\end{aligned} \tag{S2}$$

The CF Hamiltonian $\hat{\mathcal{H}}_{CF}$ splits those orbitals by Δ and the SO Hamiltonian takes the simple form $\hat{h}_{SO} = \zeta\, \hat{\boldsymbol{L}}\boldsymbol{.}\hat{\boldsymbol{S}}$ where $\hat{\boldsymbol{L}}$ and $\hat{\boldsymbol{S}}$ are the total electronic angular and spin momenta operators respectively and ζ is the SOC constant and is positive. We have recently shown that the ordering of the $4f$ orbitals in lanthanocenes is $4f_\sigma < 4f_\pi < 4f_\phi < 4f_\delta$ (δ and ϕ for $|M_L| = 2$ and 3 respectively) due to an interplay of electrostatic and covalent effects. This ordering is the same as

in $[U(\eta^7\text{-}C_7H_7)_2]^-$. Δ is positive for electrostatic reasons, because the two COT rings create an oblate environment.

The representation of the model Hamiltonian $\hat{h} = \hat{h}_{CF} + \hat{h}_{SO}$ in the set of CF functions of Eqs. S2 is

$$\begin{array}{c|cc} \hat{h} & \left|\sigma_{1/2}\right\rangle & \left|\pi_{1/2}\right\rangle \\ \hline \left\langle\sigma_{1/2}\right| & -\frac{1}{2}\Delta & \sqrt{3}\zeta \\ \left\langle\pi_{1/2}\right| & \sqrt{3}\zeta & \frac{1}{2}\Delta - \frac{1}{2}\zeta \end{array} \tag{S3}$$

and in the set of free ion functions S1

$$\begin{array}{c|cc} \hat{h} & \left|\frac{5}{2},\frac{1}{2}\right\rangle & \left|\frac{7}{2},\frac{1}{2}\right\rangle \\ \hline \left\langle\frac{5}{2},\frac{1}{2}\right| & \frac{1}{14}\Delta - 2\zeta & \frac{2\sqrt{3}}{7}\Delta \\ \left\langle\frac{7}{2},\frac{1}{2}\right| & \frac{2\sqrt{3}}{7}\Delta & -\frac{1}{14}\Delta + \frac{3}{2}\zeta \end{array} \tag{S4}$$

The ground doublet composition is obtained by diagonalizing these equivalent matrices; within a CF perspective, it is written as

$$\begin{array}{rcl} \left|\Psi\right\rangle & = & a\left|\sigma_{1/2}\right\rangle - b\left|\pi_{1/2}\right\rangle = af_\sigma - b\bar{f}_{\pi+} \\ \left|\bar{\Psi}\right\rangle & = & \mathcal{K}\left|\Psi\right\rangle = a\left|\sigma_{-1/2}\right\rangle - b\left|\pi_{-1/2}\right\rangle \\ & = & a\bar{f}_\sigma - bf_{\pi-} \end{array} \tag{S5}$$

where $\mathcal{K}$ is the time reversal operator and in a free ion perspective,

$$\begin{array}{rcl} \left|\Psi\right\rangle & = & A\left|\frac{5}{2},\frac{1}{2}\right\rangle - B\left|\frac{7}{2},\frac{1}{2}\right\rangle \\ \left|\bar{\Psi}\right\rangle & = & A\left|\frac{5}{2},-\frac{1}{2}\right\rangle - B\left|\frac{7}{2},-\frac{1}{2}\right\rangle \end{array} \tag{S6}$$

where a, b, A and B are positive real numbers with $a^2 + b^2 = A^2 + B^2 = 1$.

The orbital and spin contributions to the g factors are given by[5]

$$\begin{array}{rcl} g_\parallel^L & = & 2\left\langle\Psi\left|\hat{L}_z\right|\Psi\right\rangle = 2\,b^2 \\ g_\parallel^S & = & 4\left\langle\Psi\left|\hat{S}_z\right|\Psi\right\rangle = 2\,(a^2 - b^2) \\ g_\perp^L & = & 2\,\mathrm{Re}\left\langle\Psi\left|\hat{L}_x\right|\bar{\Psi}\right\rangle = -4\sqrt{3}\,ab \\ g_\perp^S & = & 4\,\mathrm{Re}\left\langle\Psi\left|\hat{S}_x\right|\bar{\Psi}\right\rangle = 2\,a^2 \end{array} \tag{S7}$$

These expressions were already given by Abragam and Bleaney[6] and Gourier.[3] The contributions to g are represented in Figure S3 as a function of $x = \zeta/\Delta$, as well as a and b. In this first approach, the SOC couples the CF states. At the limit of vanishing SOC, $\zeta = x = b = 0$, the ground state is the pure spin doublet $^2A_{2u}$ with $a = 1$. g factors are isotropic and equal to 2. SOC couples f_σ with $\bar{f}_{\pi+}$; it decreases the spin contribution, introduces orbital magnetization by first order contribution $\left\langle f_{\pi+}\left|\hat{l}_\parallel\right|f_{\pi+}\right\rangle$ in $g_\parallel$ and coupling contribution $\left\langle f_\sigma\left|\hat{l}_\perp\right|f_{\pi+}\right\rangle$ in $g_\perp$. Eq. S4 describes the coupling within another perspective, as the coupling of the free ion states $\left|\frac{5}{2},\frac{1}{2}\right\rangle$ and $\left|\frac{7}{2},\frac{1}{2}\right\rangle$ by CF operator. In the limit of no CF, $x \to 0$, one obtains the g factors of the free ion, $g_\parallel = 6/7$ and $g_\perp = -18/7$. According to CASSCF calculations on the monomer with PT2 geometry, $\zeta = 667$ cm^{-1}, $\Delta = 491$ cm^{-1} which gives $x = 0.736$, $a = 0.731$, $b = 0.683$, $A = 0.994$ and $B = 0.105$. These parameters are given in Table 2 for other geometries. It shows that the ground state of the monomer is close to the $\left|\frac{5}{2},\pm\frac{1}{2}\right\rangle$ spinors of the free ion and that the effect of the ligands can be modeled as a coupling with the excited $\left|\frac{7}{2},\pm\frac{1}{2}\right\rangle$ spinors. It should be noted that x is also close to 1 in $[U(\eta^7\text{-}C_7H_7)_2]^-$, while in this actinide complex, both ζ and Δ are much

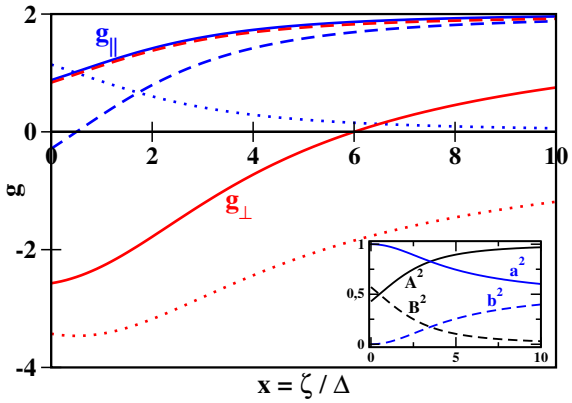

Figure S3: $g_{\parallel}$(blue), $g_{\perp}$(red) with respect to $x = \zeta/\Delta$. g^L and g^S contributions are given in dotted and dashed lines respectively (see Eqs. S7). Insert: Composition of the ground state with respect to x (see Eqs. S5 and S6).

larger, the former due to larger relativistic effects, the latter due to larger covalent interaction between $5f$ orbitals with those of the ligands. The results are close to the free ion limit, as it was the case for $[U(\eta^7\text{-}C_7H_7)_2]^-$ and in the AcX_6 series.

While only the product of the three g factors is defined and is positive, it leads to an undefined sign for $g_{\perp}$. One may assign a sign to $g_{\perp}$ by constraining the two spinors of the KD to behave under the rotations of the molecule as a real spin doublet, to within a scalar function.[7, 4, 8, 9] The sign of the g factors may be determined by constraining the set of wave functions of the model space to behave under the rotations of the molecular systems as the corresponding real spin.[7, 8] In the case of doublets, in octahedral $5f^1$, the sign of g was unequivocally assigned[4] but for a yle complex, the sign of the perpendicular g factor was undefined;[10] in the case of an octahedral quartet, two sets of g factors were compatible with rotation symmetries.[11] In the present case, the ground KD spans $E_{1/2u}$ symmetry while a spin doublet spans the $E_{1/2g}$ irrep. Since $E_{1/2u} = A_{1u} \otimes E_{1/2g}$ and $E_{1/2u} = A_{2u} \otimes E_{1/2g}$, the scalar function may be either A_{1u} or A_{2u}. With A_{1u}, the two components of the KD are $|\mathcal{D}, +\rangle = i\,|\Psi\rangle$ and $|\mathcal{D}, -\rangle = -i\,|\bar{\Psi}\rangle$ where $|\Psi\rangle$ and $|\bar{\Psi}\rangle$ are given in Eqs. S5 which leads to $g_{\perp} = 2\ \mathrm{Re}\left\langle \mathcal{D}, + \left| \hat{L}_x + 2\hat{S}_x \right| \mathcal{D}, - \right\rangle = -2a^2 + 4\sqrt{3}ab$. With A_{2u}, the two components of the KD are $|\mathcal{D}, +\rangle = |\Psi\rangle$ and $|\mathcal{D}, -\rangle = |\bar{\Psi}\rangle$ which leads to the opposite value of $g_{\perp} = 2a^2 - 4\sqrt{3}ab$. It means that this is not sufficient to determine the sign of $g_{\perp}$. If one adds the condition that the CF limit with $x = 0$ is a ${}^2A_{2u}$ term, it is in favor of the second solution which leads for $b = 0$ to three identical g factors $g = 2$, to the contrary of the first solution which leads to two negative factors. Choosing the A_{2u} scalar function, one gets $g_{\perp}$ as represented in Figure S3 and for $x \approx 1$, $g_{\perp}$ is negative.

S4.2 Spin Hamiltonian for the dimer

The ground state of each monomer, denoted A and B, is a KD of symmetry $M_J = \pm\frac{1}{2}$ well separated in energy from the first excited KD; the model space for each monomer is the ground KD and the local pseudo-spins are $\mathbb{S}_A = 1/2$ and $\mathbb{S}_B = 1/2$ with the corresponding states $|\mathcal{D}, \pm\rangle^A$ and $|\mathcal{D}, \pm\rangle^B$. The model space of the dimer is of dimension four and is generated by the set $|\mathcal{D}, \pm\rangle^A \otimes |\mathcal{D}, \pm\rangle^B$. The derivation of the spin Hamiltonian for the dimer follows the traditional one, replacing spin operators by pseudo-spin operators.[12] The local spin Hamiltonians are, with

an external magnetic field $\boldsymbol{B}$

$$\begin{aligned}\hat{\mathcal{H}}_S^X &= \mu_B \boldsymbol{B} \,.\, \mathbf{g} \,.\, \hat{\mathbb{S}}^X \\ &= \mu_B \left(B_x g_\perp \hat{\mathbb{S}}_x^X + B_y g_\perp \hat{\mathbb{S}}_y^X + B_z g_\parallel \hat{\mathbb{S}}_z^X \right) \\ &= \gamma_\perp \hat{\mathbb{S}}_x^X + \gamma_\perp \hat{\mathbb{S}}_y^X + \gamma_\parallel \hat{\mathbb{S}}_z^X \end{aligned} \tag{S8}$$

with $X = A, B$, B_u the component of the field in direction u and $\gamma_u = \mu_B g_u B_u$. The Hamiltonian describing the interaction between the two magnetic sites may be written using tensor $\mathbf{D}^{AB}$

$$\begin{aligned}\hat{\mathcal{H}}_S^{AB} &= \hat{\mathbb{S}}^A \,.\, \mathbf{D}^{AB} \,.\, \hat{\mathbb{S}}^B \\ &= -J\, \hat{\mathbb{S}}^A \,.\, \hat{\mathbb{S}}^B + D \left[\hat{\mathbb{S}}_z^A \hat{\mathbb{S}}_z^B - \frac{1}{3} \hat{\mathbb{S}}^A \,.\, \hat{\mathbb{S}}^B \right] \\ &\quad + E \left[\hat{\mathbb{S}}_x^A \hat{\mathbb{S}}_x^B - \hat{\mathbb{S}}_y^A \hat{\mathbb{S}}_y^B \right] \end{aligned} \tag{S9}$$

where the isotropic interaction is characterized by J (Heisenberg Hamiltonian) and the anisotropic coupling by the two parameters D and E. The total Hamiltonian

$$\hat{\mathcal{H}}_S = \hat{\mathcal{H}}_S^A + \hat{\mathcal{H}}_S^B + \hat{\mathcal{H}}_S^{AB} \tag{S10}$$

written in the basis set of the local spin functions

$$\begin{aligned} |\pm\pm\rangle &= |\mathcal{D}, \pm\rangle^A \otimes |\mathcal{D}, \pm\rangle^B \\ |\pm\mp\rangle &= |\mathcal{D}, \pm\rangle^A \otimes |\mathcal{D}, \mp\rangle^B \end{aligned} \tag{S11}$$

gives rise to the following representation matrix

$\hat{\mathcal{H}}_S$	$\lvert{+}{+}\rangle$	$\lvert{+}{-}\rangle$	$\lvert{-}{+}\rangle$	$\lvert{-}{-}\rangle$
$\langle{+}{+}\rvert$	$-\frac{J}{4} + \frac{D}{6} + \gamma_z$	$\frac{\gamma_x - i\gamma_y}{2}$	$\frac{\gamma_x - i\gamma_y}{2}$	$\frac{E}{2}$
$\langle{+}{-}\rvert$	$\frac{\gamma_x + i\gamma_y}{2}$	$\frac{J}{4} - \frac{D}{6}$	$-\frac{J}{2} - \frac{D}{6}$	$\frac{\gamma_x - i\gamma_y}{2}$
$\langle{-}{+}\rvert$	$\frac{\gamma_x + i\gamma_y}{2}$	$-\frac{J}{2} - \frac{D}{6}$	$\frac{J}{4} - \frac{D}{6}$	$\frac{\gamma_x - i\gamma_y}{2}$
$\langle{-}{-}\rvert$	$\frac{E}{2}$	$\frac{\gamma_x + i\gamma_y}{2}$	$\frac{\gamma_x + i\gamma_y}{2}$	$-\frac{J}{4} + \frac{D}{6} - \gamma_z$

(S12)

The eigenstates of the total pseudo-spin operator $\hat{\mathbb{S}} = \hat{\mathbb{S}}_A + \hat{\mathbb{S}}_B$ form either a pseudo-singlet

$$|\mathcal{S}, 0\rangle = \frac{1}{\sqrt{2}} \left(|{+}{-}\rangle - |{-}{+}\rangle \right) \tag{S13}$$

or a -triplet,

$$\begin{aligned} |\mathcal{T}, 1\rangle &= |{+}{+}\rangle \\ |\mathcal{T}, 0\rangle &= \frac{1}{\sqrt{2}} \left(|{+}{-}\rangle + |{-}{+}\rangle \right) \\ |\mathcal{T}, -1\rangle &= |{-}{-}\rangle \end{aligned} \tag{S14}$$

The matrix of Eq. S12 becomes in this new basis

$\hat{\mathcal{H}}_S$	$\lvert\mathcal{S}, 0\rangle$	$\lvert\mathcal{T}, 1\rangle$	$\lvert\mathcal{T}, 0\rangle$	$\lvert\mathcal{T}, -1\rangle$
$\langle\mathcal{S}, 0\rvert$	$\frac{3J}{4}$	0	0	0
$\langle\mathcal{T}, 1\rvert$	0	$-\frac{J}{4} + \frac{D}{6} + \gamma_z$	$\frac{\gamma_x - i\gamma_y}{\sqrt{2}}$	$\frac{E}{2}$
$\langle\mathcal{T}, 0\rvert$	0	$\frac{\gamma + i\gamma_y}{\sqrt{2}}$	$-\frac{J}{4} - \frac{D}{3}$	$\frac{\gamma_x - i\gamma_y}{\sqrt{2}}$
$\langle\mathcal{T}, -1\rvert$	0	$\frac{E}{2}$	$\frac{\gamma_x + i\gamma_y}{\sqrt{2}}$	$-\frac{J}{4} + \frac{D}{6} + \gamma_z$

(S15)

This matrix is the representation of the Spin Hamiltonian expressed with the total -spin $\hat{\mathbf{S}}$

$$\begin{aligned}\hat{\mathcal{H}}_S &= -\frac{1}{2}J\hat{\mathbf{S}}^2+\frac{3}{4}J+\frac{1}{2}D\left[\hat{\mathbb{S}}_z^2-\frac{1}{3}\hat{\mathbf{S}}^2\right]\\ &\quad+\frac{1}{2}E\left[\hat{\mathbb{S}}_x^2-\hat{\mathbb{S}}_y^2\right]+\gamma_x\hat{\mathbb{S}}_x+\gamma_y\hat{\mathbb{S}}_y+\gamma_z\hat{\mathbb{S}}_z\end{aligned} \tag{S16}$$

which can be rewritten using new ZFS and g tensors $\mathbf{D}$ and $\mathbf{G}$

$$\hat{\mathcal{H}}_S = \hat{\mathbf{S}}\,.\,\mathbf{D}\,.\,\hat{\mathbf{S}}+\mu_B\boldsymbol{B}\,.\,\mathbf{G}\,.\,\hat{\mathbf{S}} \tag{S17}$$

All parameters of Eq. S16 can be deduced from first principle calculation on the dimer: SO-RASSI calculation provides wave functions which diagonalize the Zero-Field Hamiltonian and the four low lying wave functions $\{|\Psi_1\rangle,|\Psi_2\rangle,|\Psi_3\rangle,|\Psi_4\rangle\}$ have energies E_i. The three 4*4 matrices of the total angular moment $\hat{\boldsymbol{m}}=-\mu_B\left(\hat{\boldsymbol{L}}+g_e\hat{\boldsymbol{S}}\right)$ are calculated in this basis set and denoted $\mathbf{M}_x$, $\mathbf{M}_y$ and $\mathbf{M}_z$. In order to deduce tspin Hamiltonian parameters from first principle calculations, the correspondence between these four wave functions to the four spin states needs to be determined.[11] In the model space, the matrices for $\hat{m}_x$, $\hat{m}_y$ and $\hat{m}_z$ are

$\hat{m}_x$	$\lvert\mathcal{S},0\rangle$	$\lvert\mathcal{T},1\rangle$	$\lvert\mathcal{T},0\rangle$	$\lvert\mathcal{T},-1\rangle$
$\langle\mathcal{S},0\rvert$	0	0	0	0
$\langle\mathcal{T},1\rvert$	0	0	$\frac{1}{\sqrt{2}}G_\perp$	0
$\langle\mathcal{T},0\rvert$	0	$\frac{1}{\sqrt{2}}G_\perp$	0	$\frac{1}{\sqrt{2}}G_\perp$
$\langle\mathcal{T},-1\rvert$	0	0	$\frac{1}{\sqrt{2}}G_\perp$	0

(S18)

$\hat{m}_y$	$\lvert\mathcal{S},0\rangle$	$\lvert\mathcal{T},1\rangle$	$\lvert\mathcal{T},0\rangle$	$\lvert\mathcal{T},-1\rangle$
$\langle\mathcal{S},0\rvert$	0	0	0	0
$\langle\mathcal{T},1\rvert$	0	0	$-\frac{i}{\sqrt{2}}G_\perp$	0
$\langle\mathcal{T},0\rvert$	0	$\frac{i}{\sqrt{2}}G_\perp$	0	$-\frac{i}{\sqrt{2}}G_\perp$
$\langle\mathcal{T},-1\rvert$	0	0	$\frac{i}{\sqrt{2}}G_\perp$	0

(S19)

$\hat{m}_z$	$\lvert\mathcal{S},0\rangle$	$\lvert\mathcal{T},1\rangle$	$\lvert\mathcal{T},0\rangle$	$\lvert\mathcal{T},-1\rangle$
$\langle\mathcal{S},0\rvert$	0	0	0	0
$\langle\mathcal{T},1\rvert$	0	$G_\parallel$	0	0
$\langle\mathcal{T},0\rvert$	0	0	0	0
$\langle\mathcal{T},-1\rvert$	0	0	0	$-G_\parallel$

(S20)

The -singlet $|\mathcal{S},0\rangle$ is non magnetic and is easily assigned to the non-magnetic state $|\Psi_1\rangle$ with energy E_1. The diagonalization of $\hat{m}_z$ in $\{|\Psi_2\rangle,|\Psi_3\rangle,|\Psi_4\rangle\}$ space gives eigenvalues 0 and $\pm G_\parallel$. $|\mathcal{T},0\rangle$ is assigned to $|\Psi_2\rangle$ the state with $M_z=0$, while the two states $|\Psi_3\rangle$ and $|\Psi_4\rangle$ with $M_z=\pm G_\parallel$ correspond to $|\mathcal{T},\pm1\rangle$ ($G_\parallel>0$) or $|\mathcal{T},\mp1\rangle$ ($G_\parallel<0$) towards a phase factor. Following the procedure of reference[11] where $\mathbf{M}_z$ is first diagonalized and either $\mathbf{M}_x$ or $\mathbf{M}_y$ is made real, one finds that both $G_\parallel$ and $G_\perp$ may be either positive or negative; this procedure does not permit to assign a sign to these parameters. But they can be determined using the rotations as in Section S4.1. In symmetry $\mathcal{D}_{8h}$, a spin $S=1$ spans the irreps $A_{2g}\oplus E_{1g}$ while the ground triplet of the dimer spans $A_{1u}\oplus E_{1u}$. The multiplying scalar function must span the one-fold irrep A_{2u} since $A_{1u}\oplus E_{1u}=A_{2u}\otimes(A_{2g}\oplus E_{1g})$. Considering the two rotations $\mathcal{C}_2^z$ and $\mathcal{C}_2^x$ of angle π about axes z and x respectively, one finds $\mathcal{C}_2^z(|\mathcal{T},0\rangle)=|\mathcal{T},0\rangle$ and $\mathcal{C}_2^x(|\mathcal{T},0\rangle)=|\mathcal{T},0\rangle$ leading to the representation matrices in basis $\{|\mathcal{T},1\rangle,|\mathcal{T},-1\rangle\}$

$$\Gamma(\mathcal{C}_2^z)=\begin{bmatrix}-1&0\\0&-1\end{bmatrix};\Gamma(\mathcal{C}_2^x)=\begin{bmatrix}0&1\\1&0\end{bmatrix} \tag{S21}$$

Since $\chi_{A_{2u}}(\mathcal{C}_2^z) = 1$; $\chi_{A_{2u}}(\mathcal{C}_2^x) = -1$, one concludes that $|\mathcal{T},0\rangle$ and $|\mathcal{T},\pm1\rangle$ as defined in Eqs. S14 behave as a real spin $S = 1$ multiplied by a scalar function of symmetry A_{2u} under the rotations of the molecules. It follows that

$$\begin{aligned} G_{\parallel} &= \left\langle \mathcal{T},1 \left| \hat{L}_z + 2\hat{S}_z \right| \mathcal{T},1 \right\rangle = 2 \left\langle \mathcal{D},+ \left| \hat{l}_z + 2\hat{s}_z \right| \mathcal{D},+ \right\rangle = g_{\parallel} \\ G_{\perp} &= \sqrt{2} \left\langle \mathcal{T},0 \left| \hat{L}_x + 2\hat{S}_x \right| \mathcal{T},1 \right\rangle = 2 \left\langle \mathcal{D},- \left| \hat{l}_x + 2\hat{s}_x \right| \mathcal{D},+ \right\rangle = g_{\perp} \end{aligned} \tag{S22}$$

and $G_{\parallel}$ and $G_{\perp}$ equal $g_{\parallel}$ and $g_{\perp}$ within the limit of vanishing interaction between the two magnetic centers, and consequently have the same sign.

Values of $G_{\parallel}$ and $G_{\perp}$ deduced from RASSI calculations are summarized in Table S4. As for the monomer (see Table S1), the values show almost no dependency on both structure and correlation, and the values for the dimer the same as for the monomer. This confirms the local nature of the g values. Orbital and spin contributions are evaluated as $G_{\parallel}^L = \left\langle \mathcal{T},1 \left| \hat{L}_z \right| \mathcal{T},1 \right\rangle$, $G_{\parallel}^S = \left\langle \mathcal{T},1 \left| 2\hat{S}_z \right| \mathcal{T},1 \right\rangle$, $G_{\perp}^L = \sqrt{2} \left\langle \mathcal{T},0 \left| \hat{L}_x \right| \mathcal{T},1 \right\rangle$ and $G_{\perp}^S = \sqrt{2} \left\langle \mathcal{T},0 \left| 2\hat{S}_x \right| \mathcal{T},1 \right\rangle$. The parallel contributions are both positive while spin and orbit perpendicular ones are opposite in signs, the orbit one being the largest. This matches with Eqs. S7. $G_{\perp}^S$ arises only from the σ state while $G_{\parallel}^S$ is reduced due to the π contribution. $G_{\parallel}^L$ arises only from the π state while $G_{\perp}^L$ is due to the coupling between σ and π states.

Table S4: g factors for the ground pseudo-triplet of $[Ce_2(COT)_3]$ as defined in Section S4.2 calculated with CI methods for the three structures of Table 1. S and L denote spin and orbital contributions.

struct	meth	$G_{\parallel}$	$G_{\perp}$	$G_{\parallel}^S$	$G_{\perp}^S$	$G_{\parallel}^L$	$G_{\perp}^L$
EXAFS	CASCI	1.079	-2.344	0.164	1.082	0.914	-3.429
	CAS+S	1.100	-2.319	0.206	1.102	0.893	-3.421
	DDCI2	1.103	-2.308	0.212	1.112	0.891	-3.420
	DDCI3	1.100	-2.309	0.206	1.112	0.893	-3.421
PT2	CASCI	1.061	-2.370	0.064	1.064	0.932	-3.434
	CAS+S	1.077	-2.349	0.160	1.080	0.916	-3.429
	DDCI2	1.079	-2.346	0.164	1.082	0.914	-3.428
	DDCI3	1.078	-2.349	0.162	1.080	0.915	-3.429
DFT	CASCI	1.052	-2.389	0.108	1.054	0.943	-3.443
	CAS+S	1.065	-2.374	0.114	1.066	0.930	-3.440
	DDCI2	1.067	-2.370	0.138	1.070	0.928	-3.440
	DDCI3	1.066	-2.370	0.138	1.070	0.928	-3.440

S4.3 Model Hamiltonian for the dimer

In the dimer, the model Hamiltonian which describes the two magnetic electrons may be written as

$$\hat{\mathcal{H}} = \hat{h}^A + \hat{h}^B + \hat{h}^{AB} + \frac{1}{r_{12}} + \zeta\, \hat{\boldsymbol{l}}^A \cdot \hat{\boldsymbol{s}}^A + \zeta\, \hat{\boldsymbol{l}}^B \cdot \hat{\boldsymbol{s}}^B \tag{S23}$$

where $\hat{h}_{A/B}$ is the one-center one-electron Hamiltonian, $\hat{h}_{AB}$ is the one-electron coupling term, $\frac{1}{r_{12}}$ is the electron-electron repulsion and $\zeta \hat{\boldsymbol{l}}^{A/B} \cdot \hat{\boldsymbol{s}}^{A/B}$ is the local SOC operator. Following the approach of reference 13, we introduce the bonding and antibonding combinations of σ and π

spin-orbitals

$$\begin{aligned}
\sigma &= \frac{1}{\sqrt{2}}\left(f_\sigma^A - f_\sigma^B\right) \quad ; \quad \bar{\sigma} = \frac{1}{\sqrt{2}}\left(\bar{f}_\sigma^A - \bar{f}_\sigma^B\right) \\
\sigma^* &= \frac{1}{\sqrt{2}}\left(f_\sigma^A + f_\sigma^B\right) \quad ; \quad \bar{\sigma}^* = \frac{1}{\sqrt{2}}\left(\bar{f}_\sigma^A + \bar{f}_\sigma^B\right) \\
\pi_{-1} &= \frac{1}{\sqrt{2}}\left(f_{\pi-}^A + f_{\pi-}^B\right) = \frac{1}{\sqrt{2}}\left(\pi_x - i\pi_y\right) \\
\bar{\pi}_1 &= \frac{1}{\sqrt{2}}\left(\bar{f}_{\pi+}^A + \bar{f}_{\pi+}^B\right) = \frac{1}{\sqrt{2}}\left(-\bar{\pi}_x - i\bar{\pi}_y\right) \\
\pi_{-1}^* &= \frac{1}{\sqrt{2}}\left(f_{\pi-}^A - f_{\pi-}^B\right) = \frac{1}{\sqrt{2}}\left(\pi_x^* - i\pi_y^*\right) \\
\bar{\pi}_1^* &= \frac{1}{\sqrt{2}}\left(\bar{f}_{\pi+}^A - \bar{f}_{\pi+}^B\right) = \frac{1}{\sqrt{2}}\left(-\bar{\pi}_x^* - i\bar{\pi}_y^*\right)
\end{aligned} \tag{S24}$$

where unbarred and barred orbitals denote α and β spin contributions respectively, $f_m^{A/B}$ denote the $4f$ orbital localized on A/B with angular part being the spherical harmonics $Y_{3,m}$. The real orbitals are defined as $f_x^{A/B} = \frac{1}{\sqrt{2}}\left(f_{\pi+}^{A/B} - f_{\pi-}^{A/B}\right)$ and $f_y^{A/B} = \frac{i}{\sqrt{2}}\left(f_{\pi+}^{A/B} + f_{\pi-}^{A/B}\right)$. Two-electron wave functions are built with those spin-orbitals. Without SOC, states are denoted according to spin multiplicity (S and T for singlet and triplet respectively, and spin projection M), to spatial inversion and to the configuration of the two electrons in σ and π orbitals. States are either neutral with one electron on each site or ionic with the two electrons on one site; the latter are denoted with superscript *ion*. For example, $|T_u^{\sigma\pi}, 1\rangle$ is a ungerade spin triplet with $M_S = 1$, with determinants of type $\left\{f_\sigma^A f_\pi^B\right\}$ (the $\{\}$ denotes the $A \leftrightarrow B$ symmetrization) and $\left|T_u^{\sigma\pi,ion}, 0\right\rangle$ a ungerade spin triplet state with $M_S = 0$ built with determinants of type $\left\{f_\sigma^A f_\pi^A\right\}$.

The $\sigma\sigma$ configuration leads to the well-known neutral spin singlet and triplet states and to the ionic singlet.

$$\begin{aligned}
\left|S_g^{\sigma\sigma}, 0\right\rangle &= \frac{1}{\sqrt{2}}\left(|\sigma\bar{\sigma}| - |\sigma^*\bar{\sigma}^*|\right) = \frac{1}{\sqrt{2}}\left(-\left|f_\sigma^A \bar{f}_\sigma^B\right| + \left|\bar{f}_\sigma^A f_\sigma^B\right|\right) \\
|T_u^{\sigma\sigma}, 0\rangle &= \frac{1}{\sqrt{2}}\left(|\sigma\bar{\sigma}^*| + |\bar{\sigma}\sigma^*|\right) = \frac{1}{\sqrt{2}}\left(\left|f_\sigma^A \bar{f}_\sigma^B\right| + \left|\bar{f}_\sigma^A f_\sigma^B\right|\right) \\
|T_u^{\sigma\sigma}, 1\rangle &= |\sigma\sigma^*| = \left|f_\sigma^A f_\sigma^B\right| \\
|T_u^{\sigma\sigma}, -1\rangle &= |\bar{\sigma}\bar{\sigma}^*| = \left|\bar{f}_\sigma^A \bar{f}_\sigma^B\right| \\
\left|S_g^{\sigma\sigma,ion}, 0\right\rangle &= \frac{1}{\sqrt{2}}\left(|\sigma\bar{\sigma}| + |\sigma^*\bar{\sigma}^*|\right) = \frac{1}{\sqrt{2}}\left(\left|f_\sigma^A \bar{f}_\sigma^A\right| + \left|\bar{f}_\sigma^B f_\sigma^B\right|\right)
\end{aligned} \tag{S25}$$

$\left|S_g^{\sigma\sigma}, 0\right\rangle$ is the zeroth order *ab initio* counterpart of the pseudo-singlet $|\mathcal{S}, 0\rangle$. It couples to different excited states as given in the following matrix

$\hat{\mathcal{H}}$	$\left\|S_g^{\sigma\sigma}, 0\right\rangle$	$\left\|T_g^{\sigma\pi}, \pm1\right\rangle$	$\left\|S_g^{\pi\pi}, 0\right\rangle$	$\left\|S_g^{\sigma\sigma,ion}, 0\right\rangle$	$\left\|T_g^{\sigma\pi,ion}, \pm1\right\rangle$	$\left\|S_g^{\pi\pi,ion}, 0\right\rangle$
$\left\langle S_g^{\sigma\sigma}, 0\right\|$	0	$\sqrt{6}\zeta$	0	$2\beta^\sigma$	0	0
$\left\langle T_g^{\sigma\pi}, \pm1\right\|$	$\sqrt{6}\zeta$	$\Delta + k_{00}^{\sigma\pi} - \frac{1}{2}\zeta$	$\sqrt{6}\zeta$	0	$\beta^\sigma + \beta^\pi$	0
$\left\langle S_g^{\pi\pi}, 0\right\|$	0	$\sqrt{6}\zeta$	$2\Delta - \zeta$	0	0	$2\beta^\pi$
$\left\langle S_g^{\sigma\sigma,ion}, 0\right\|$	$2\beta^\sigma$	0	0	U	0	0
$\left\langle T_g^{\sigma\pi,ion}, \pm1\right\|$	0	$\beta^\sigma + \beta^\pi$	0	0	$U - K^U$	0
$\left\langle S_g^{\pi\pi,ion}, 0\right\|$	0	0	$2\beta^\pi$	0	0	U

(S26)

Δ is an effective CF parameter taking into account the difference between two-electron interactions

$$\Delta = \varepsilon^\pi - \varepsilon^\sigma + J^{\sigma\pi} - J^{\sigma\sigma} = \varepsilon^\pi - \varepsilon^\sigma + J^{\pi\pi} - J^{\sigma\pi} \tag{S27}$$

where $\varepsilon^\sigma = \left\langle f_\sigma^{A/B} \middle| \hat{h}_{A/B} \middle| f_\sigma^{A/B} \right\rangle$ and $\varepsilon^\pi = \left\langle f_{\pi_{x/y}}^{A/B} \middle| \hat{h}_{A/B} \middle| f_{\pi_{x/y}}^{A/B} \right\rangle$ are the one-site energies, $J^{\sigma\sigma} = \left[f_\sigma^A f_\sigma^A | f_\sigma^B f_\sigma^B\right]$ and $J^{\sigma\pi} = \left[f_\sigma^A f_\sigma^A | f_{\pi_x}^B f_{\pi_x}^B\right]$ Coulomb integrals defined with Mulliken notations, $\beta^{\sigma\sigma} = \left\langle f_\sigma^A \middle| \hat{h}_{AB} \middle| f_\sigma^B \right\rangle$ and $\beta^{\sigma\pi} = \left\langle f_\sigma^A \middle| \hat{h}_{AB} \middle| f_{\pi_{x,y}}^B \right\rangle = \left\langle f_\sigma^B \middle| \hat{h}_{AB} \middle| f_{\pi_{x,y}}^A \right\rangle$ the hopping integrals between sites A and B, U is the one-site Coulomb repulsion energy and is considered to be independent of the occupied orbitals and K^U is the one-site exchange energy, again considered to be independent of the orbitals. $k_{00}^{\sigma\pi}$ is the two-electron contribution specific to state $\left|T_g^{\sigma\pi}, \pm 1\right\rangle$ which is a combination of $\left|T_g^{\sigma\pi}, 1\right\rangle$ and $\left|T_g^{\sigma\pi}, -1\right\rangle$.

Similarly, $|T_u^{\sigma\sigma}, M_S\rangle$ are the *ab initio* zeroth order counterparts of the three components of the pseudo-triplet $|\mathcal{T}, \mathbb{M}\rangle$. The coupling matrices for these states are

$\hat{\mathcal{H}}$	$\lvert T_u^{\sigma\sigma}, 0\rangle$	$\lvert T_u^{\sigma\pi}, \pm 1\rangle$	$\lvert T_u^{\pi\pi}, 0\rangle$	$\left\lvert T_u^{\sigma\pi,ion}, \pm 1\right\rangle$
$\langle T_u^{\sigma\sigma}, 0\rvert$	$-K^{\sigma\sigma}$	$\sqrt{6}\zeta$	0	0
$\langle T_u^{\sigma\pi}, \pm 1\rvert$	$\sqrt{6}\zeta$	$\Delta + k_{10}^{\sigma\pi} - \frac{1}{2}\zeta$	$\sqrt{6}\zeta$	$\beta^\sigma - \beta^\pi$
$\langle T_u^{\pi\pi}, 0\rvert$	0	$\sqrt{6}\zeta$	$2\Delta - \zeta$	0
$\left\langle T_u^{\sigma\pi,ion}, \pm 1\right\rvert$	0	$\beta^\sigma - \beta^\pi$	0	$U - K^U$

(S28)

$\hat{\mathcal{H}}$	$\lvert T_u^{\sigma\sigma}, 1\rangle$	$\lvert ST_u^{\sigma\pi}, 0\rangle$	$\lvert T_u^{\pi\pi}, \pm 1\rangle$	$\left\lvert ST_u^{\sigma\pi,ion}, 0\right\rangle$
$\langle T_u^{\sigma\sigma}, 1\rvert$	$-K^{\sigma\sigma}$	$\sqrt{6}\zeta$	0	0
$\langle ST_u^{\sigma\pi}, 0\rvert$	$\sqrt{6}\zeta$	$\Delta + k_{11}^{\sigma\pi} - \frac{1}{2}\zeta$	$\sqrt{6}\zeta$	$\beta^\sigma - \beta^\pi$
$\langle T_u^{\pi\pi}, \pm 1\rvert$	0	$\sqrt{6}\zeta$	$2\Delta - \zeta$	0
$\left\langle ST_u^{\sigma\pi,ion}, 0\right\rvert$	0	$\beta^\sigma - \beta^\pi$	0	$U - \frac{1}{2}K^U$

(S29)

$|T_u^{\sigma\pi}, \pm 1\rangle$ is a combination of $|T_u^{\sigma\pi}, 1\rangle$ and $|T_u^{\sigma\pi}, -1\rangle$, $|T_u^{\pi\pi}, \pm 1\rangle$ of $|T_u^{\pi\pi}, 1\rangle$ and $|T_u^{\pi\pi}, -1\rangle$ and $|ST_u^{\sigma\pi}, 0\rangle$ of $|S_u^{\sigma\pi}, 0\rangle$ and $|T_u^{\sigma\pi}, 0\rangle$. $K^{\sigma\sigma} = \left[f_\sigma^A f_\sigma^B | f_\sigma^B f_\sigma^A\right]$ is the exchange integral between the local σ orbitals. Since $\zeta \approx \Delta$, it is not possible to make any pertubative development of the SOC but the effect of the ionic states may be taken into account using pertubative theory. The effective perturbation of the ionic states into the model space of the neutral states, Eqs. S26, S28 and S29 becom

$\hat{\mathcal{H}}_{eff}$	$\left\lvert S_g^{\sigma\sigma}, 0\right\rangle$	$\left\lvert T_g^{\sigma\pi}, \pm 1\right\rangle$	$\left\lvert S_g^{\pi\pi}, 0\right\rangle$
$\left\langle S_g^{\sigma\sigma}, 0\right\rvert$	$-\frac{4\beta^{\sigma\,2}}{U}$	$\sqrt{6}\zeta$	0
$\left\langle T_g^{\sigma\pi}, \pm 1\right\rvert$	$\sqrt{6}\zeta$	$\Delta + k_{00}^{\sigma\pi} - \frac{(\beta^\sigma + \beta^\pi)^2}{U - K^U} - \frac{1}{2}\zeta$	$\sqrt{6}\zeta$
$\left\langle S_g^{\pi\pi}, 0\right\rvert$	0	$\sqrt{6}\zeta$	$2\Delta - \frac{4\beta^{\pi\,2}}{U} - \zeta$

(S30)

$\hat{\mathcal{H}}_{eff}$	$\lvert T_u^{\sigma\sigma}, 0\rangle$	$\lvert T_u^{\sigma\pi}, \pm 1\rangle$	$\lvert T_u^{\pi\pi}, 0\rangle$
$\langle T_u^{\sigma\sigma}, 0\rvert$	$-K^{\sigma\sigma}$	$\sqrt{6}\zeta$	0
$\langle T_u^{\sigma\pi}, \pm 1\rvert$	$\sqrt{6}\zeta$	$\Delta + k_{10}^{\sigma\pi} - \frac{(\beta^\sigma - \beta^\pi)^2}{U - K^U} - \frac{1}{2}\zeta$	$\sqrt{6}\zeta$
$\langle T_u^{\pi\pi}, 0\rvert$	0	$\sqrt{6}\zeta$	$2\Delta - \zeta$

(S31)

$\hat{\mathcal{H}}_{eff}$	$\lvert T_u^{\sigma\sigma}, 1\rangle$	$\lvert ST_u^{\sigma\pi}, 0\rangle$	$\lvert T_u^{\pi\pi}, \pm 1\rangle$
$\langle T_u^{\sigma\sigma}, 1\rvert$	$-K^{\sigma\sigma}$	$\sqrt{6}\zeta$	0
$\langle ST_u^{\sigma\pi}, 0\rvert$	$\sqrt{6}\zeta$	$\Delta + k_{11}^{\sigma\pi} - \frac{(\beta^\sigma - \beta^\pi)^2}{U - \frac{1}{2}K^U} - \frac{1}{2}\zeta$	$\sqrt{6}\zeta$
$\langle T_u^{\pi\pi}, \pm 1\rvert$	0	$\sqrt{6}\zeta$	$2\Delta - \zeta$

(S32)

These three matrices have the common form

$$\begin{bmatrix} 0 + k_{\sigma\sigma} & \sqrt{6}\zeta & 0 \\ \sqrt{6}\zeta & \Delta - \frac{1}{2}\zeta + k_{\sigma\pi} & \sqrt{6}\zeta \\ 0 & \sqrt{6}\zeta & 2\Delta - \zeta + k_{\pi\pi} \end{bmatrix} \tag{S33}$$

where the k_i are small compared to ζ and Δ. The eigenvalues for matrix of Eq. S33 with $k_i = 0\,(i = \sigma\sigma, \sigma\pi, \pi\pi)$ are known : $2\varepsilon_\pm, \Delta - \frac{1}{2}\zeta$ with corresponding eigenvectors $\mathbf{X} = \left\{a^2, -\sqrt{2}ab, b^2\right\}$ $\left\{b^2, \sqrt{2}ab, a^2\right\}$ $\left\{\sqrt{2}ab, a^2 - b^2, -\sqrt{2}ab\right\}$ where $\varepsilon_\pm$ are the two eigenvalues of the matrix

$$\begin{bmatrix} 0 & \sqrt{3}\zeta \\ \sqrt{3}\zeta & \Delta - \frac{1}{2}\zeta \end{bmatrix} \tag{S34}$$

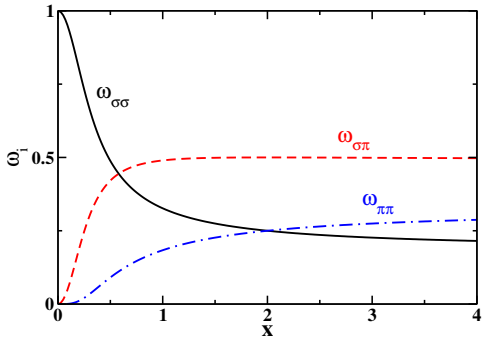

Figure S4: Dependence of the ω_i with $x = \zeta/\Delta$ as defined in Eq. S35.

with corresponding eigenvectors $\{a, -b\}$ et $\{b, a\}$. The ground energy of matrix S33 may be written as

$$E_- = 2\varepsilon_- + \omega_{\sigma\sigma} k_{\sigma\sigma} + \omega_{\sigma\pi} k_{\sigma\pi} + \omega_{\pi\pi} k_{\pi\pi} \tag{S35}$$

Within a first order Taylor expansion within the k_i, one finds $\omega_{\sigma\sigma} = a^4$, $\omega_{\sigma\pi} = 2\,a^2 b^2$ and $\omega_{\pi\pi} = b^4$ as represented as a function of $x = \zeta/\Delta$ on Figure S4.

As expected, for $x = 0$ with no SOC, $\omega_{\sigma\sigma} = 1$ and $E_- = k_{\sigma\sigma}$. Around $x \approx 1$, $\omega_{\sigma\pi}$ is the largest, $\omega_{\sigma\sigma}$ is important and $\omega_{\pi\pi}$ non negligible. The magnetic coupling is described using spin Hamiltonian of Eq. S9 with $E = 0$

$$\hat{\mathcal{H}}^{AB} = -J\,\mathbb{S}^A \cdot \mathbb{S}^B + \frac{D}{3}\left[2\,\mathbb{S}_z^A\mathbb{S}_z^B - \mathbb{S}_x^A\mathbb{S}_x^B - \mathbb{S}_y^A\mathbb{S}_y^B\right] \tag{S36}$$

Spin Hamiltonian parameters are deduced from the three lowest eigenenergies E_{00}, E_{10} and E_{11} of matrices S26, S28 and S29 respectively according to

$$\begin{aligned} J &= E_{00} - \frac{1}{3}\left(E_{10} + 2E_{11}\right) \\ D &= \frac{2}{3}\left(E_{11} - E_{10}\right) \end{aligned} \tag{S37}$$

Combining all the preceding results, one finds

$$\begin{aligned} J = \omega_{\sigma\sigma}\left[K^{\sigma\sigma} - \frac{4\beta^{\sigma\,2}}{U}\right] + \omega_{\sigma\pi}\left[k_{00}^{\sigma\pi} - \frac{1}{3}k_{10}^{\sigma\pi} - \frac{2}{3}k_{11}^{\sigma\pi}\right. \\ \left. - \frac{4\beta^\sigma\beta^\pi}{U} - \frac{K^U\left(\beta^{\sigma\,2} + 10\beta^\sigma\beta^\pi + \beta^{\pi\,2}\right)}{3U^2}\right] - \omega_{\pi\pi}\frac{4\beta^{\pi\,2}}{U} \end{aligned} \tag{S38}$$

and

$$D = \omega_{\sigma\pi}\left[\frac{2}{3}\left(k_{11}^{\sigma\pi} - k_{10}^{\sigma\pi}\right) + \left(\beta^\sigma - \beta^\pi\right)\frac{K^U}{9U^2}\right] \tag{S39}$$

J and D may be further decomposed in exchange (K) or kinetic (T) contributions for the different

configurations

$$\begin{aligned} J &= J_K^{\sigma\sigma} + J_T^{\sigma\sigma} + J_K^{\sigma\pi} + J_T^{\sigma\pi} + J_K^{\pi\pi} + J_T^{\pi\pi} \\ J_K^{\sigma\sigma} &= \omega_{\sigma\sigma} K^{\sigma\sigma} \\ J_T^{\sigma\sigma} &= -\omega_{\sigma\sigma} \frac{4\beta^{\sigma\,2}}{U} \\ J_K^{\sigma\pi} &= \omega_{\sigma\pi} \left[k_{00}^{\sigma\pi} - \frac{1}{3} k_{10}^{\sigma\pi} - \frac{2}{3} k_{11}^{\sigma\pi} \right] \\ J_T^{\sigma\pi} &= -\omega_{\sigma\pi} \left[\frac{4\beta^\sigma \beta^\pi}{U} + \frac{K^U \left(\beta^{\sigma\,2} + 10\beta^\sigma \beta^\pi + \beta^{\pi\,2} \right)}{3\,U^2} \right] \\ J_K^{\pi\pi} &\approx 0 \\ J_T^{\pi\pi} &= -\omega_{\pi\pi} \frac{4\beta^{\pi\,2}}{U} \end{aligned} \tag{S40}$$

and

$$\begin{aligned} D &= D_K^{\sigma\pi} + D_T^{\sigma\pi} \\ D_K^{\sigma\pi} &= \frac{2}{3} \omega_{\sigma\pi} \left[k_{11}^{\sigma\pi} - k_{10}^{\sigma\pi} \right] \\ D_T^{\sigma\pi} &= \omega_{\sigma\pi} \left(\beta^\sigma - \beta^\pi \right)^2 \frac{K^U}{9\,U^2} \end{aligned} \tag{S41}$$

It should be outlined that $J_K^{\pi\pi}$ is negligible because the present model neglects the difference of energy between $S_g^{\pi\pi}$ and $T_u^{\pi\pi}$ states arising from two-electron contributions.

For $x = 0$ (no SOC), $J = -\frac{4\beta^{\sigma\,2}}{U} + K^{\sigma\sigma}$ and $D = 0$; this is the usual coupling scheme between two local spins.[14, 12] The effect of SOC is the coupling with the excited π states. The matrices of Eqs S26, S28 and S29 are easily calculated from CASCI calculations where all the roots and consequently all the matrix elements may be determined. We can check at this stage that the one site repulsion energy U is almost independent on the orbital σ or π, but depends on the spin multiplicity such we may use the same U for $S_g^{\sigma\sigma,ion}$, $S_u^{\sigma\pi,ion}$ and $S_g^{\pi\pi,ion}$ and $U - K^U$ for $T_{g,u}^{\sigma\pi,ion}$. For higher levels of correlation, it is not possible to obtain the ionic states, because they are higher in energy than LMCT states and only matrices of Eqs S30, S31 and S32 in the space of the neutral configurations are known. These matrices are calculated using the effective Hamiltonian technique [15, 16] as a simple multiplication of matrices[17] which is valuable in the present case since the projection onto the model space of the neutral form is large and this does not lead to any noticeable non hermiticity of the effective Hamiltonian matrix. But the knowledge of matrices S30, S31 and S32 are not sufficient to determine all model parameters. The components of the states on the ionic determinants (of the form β/U where β and U are the coupling parameter and the one-site repulsion respectively) brings further information; it is available for $S_g^{\sigma\sigma}$ $(2\beta^\sigma/U)$, $T_g^{\sigma\pi}$ $\left((\beta^\sigma + \beta^\pi) / \left(U - K^U\right)\right)$, $S_g^{\pi\pi}$ $(2\beta^\pi/U)$ and $T_u^{\sigma\pi}$ $\left((\beta^\sigma - \beta^\pi) / \left(U - K^U\right)\right)$. But one equation is still missing and one unknown needs to be fixed. Following the work of Calzado *et al.*,[16] β^σ may be supposed to be not affected by correlation and taken to its CASCI value. We chose to keep β^π constant as well. Other parameters can be deduced and are summarized in Table S5. The SOC parameter ζ is taken from the monomer as 668 cm^{-1}.

β^σ is of some hundreds of cm^{-1} which is rather large for a $4f$ dimer; its decrease with metal-metal is very rapid, which explains the fall of the J value between the three structures. β^π is by far not negligible, and is about a quarter of the β^σ value. $K^{\sigma\sigma}$ becomes negative which has been already noted by Calzado *et al.* and was interpreted as a polarization effect. Δ, the $\sigma - \pi$ splitting, decreases slightly with the metal-metal distance as expected. It decreases at CAS+S/DDCI2 levels and increases with DDCI3 and it is larger than the corresponding parameter in the monomer (see Table 2) As shown in Eq. S27, Δ comprises a two-electron part which depends on correlation. The one-site repulsion energy decreases strongly with correlation, as expected. U is almost independent on the metal-metal distance, as expected for a one center parameter while K^U slightly decreases.

The exchange and kinetic contributions have been deduced from the model parameters according to Eqs. S40 and S41 and are given in Table S6.

Table S5: Model parameters for $[Ce_2(COT)_3]$ deduced from CI calculations. All energies in cm^{-1}.

geom/CI	β^σ	β^π	$K^{\sigma\sigma}$	Δ	U	K^U	$k_{00}^{\sigma\pi}$	$k_{10}^{\sigma\pi}$	$k_{11}^{\sigma\pi}$	$\omega_{\sigma\sigma}$	$\omega_{\sigma\pi}$	$\omega_{\pi\pi}$
DFT/CAS	236	50	0.7	608	179005	7019	0.46	0.49	-0.10	0.31	0.49	0.19
DFT/CAS+S	236	50	-0.5	558	129187	10860	-0.13	0.12	-0.20	0.30	0.49	0.20
DFT/DDCI2	236	50	-0.5	558	127558	10862	-0.22	-0.42	-0.19	0.30	0.49	0.20
DFT/DDCI3	236	50	-1.65	691	65135	3752	0.39	-0.15	0.16	0.33	0.48	0.18
PT2/CAS	447	130	2.0	564	176703	5524	-0.32	-1.12	-0.22	0.31	0.49	0.18
PT2/CAS+S	447	130	0.0	564	126431.	9077	0.02	0.74	0.04	0.30	0.49	0.20
PT2/DDCI2	447	130	0.0	566	123035	8992	-0.11	0.10	-0.22	0.30	0.49	0.20
PT2/DDCI3	447	130	-2.7	727	65274	3677	2.61	-2.46	-1.76	0.34	0.48	0.17
EXAFS/CAS	644	180	4	668	175432	4731	1.27	-1.63	-0.36	0.32	0.48	0.18
EXAFS/CAS+S	644	180	1.1	606	123008	8461	0.77	0.26	-0.24	0.31	0.49	0.19
EXAFS/DDCI2	644	180	1.1	606	121434	8494	-0.03	0.13	-0.23	0.33	0.49	0.19
EXAFS/DDCI3	644	180	-3.1	800	63883	4417	0.79	-0.98	0.83	0.36	0.48	0.16

Table S6: Exchange and kinetic contributions to J and D from Eqs. S40 and S41 for $[Ce_2(COT)_3]$ deduced from CI calculations and corresponding *ab initio* (*ai*) values from Table 4.

geom/CI	$J_K^{\sigma\sigma}$	$J_T^{\sigma\sigma}$	$J_K^{\sigma\pi}$	$J_T^{\sigma\pi}$	$J_T^{\pi\pi}$	$D_K^{\sigma\pi}$	$D_T^{\sigma\pi}$	J^{mod}	D^{mod}	J^{ai}	D^{ai}
DFT/CAS	0.22	-0.38	0.03	-0.13	-0.01	0.14	0.0003	-0.27	0.14	0.18	0.05
DFT/CAS+S	-0.14	-0.51	-0.01	-0.19	-0.01	-0.08	0.0009	-0.89	-0.08	0.93	-0.07
DFT/DDCI2	-0.15	-0.52	0.02	-0.20	-0.01	-0.05	0.0009	-0.88	-0.05	-0.91	-0.05
DFT/DDCI3	-0.55	-1.13	-0.20	-0.37	-0.02	0.06	0.001	-2.29	0.06	-2.52	0.11
PT2/CAS	0.63	-1.44	0.09	-0.66	-0.07	0.22	0.0007	-1.44	0.22	-1.28	0.06
PT2/CAS+S	0.60	-1.90	-0.12	-0.98	-0.10	-0.17	0.002	-2.52	-0.17	-3.14	-0.29
PT2/DDCI2	0.60	-1.91	-0.002	-0.98	-0.10	-0.08	0.002	-2.40	-0.07	-3.14	-0.25
PT2/DDCI3	0.68	-4.17	2.23	-1.84	-0.17	0.17	0.003	-3.27	0.17	-8.34	0.00
EXAFS/CAS	0.35	-4.40	1.01	-1.92	-0.19	0.31	0.002	-5.15	0.31	-2.83	0.07
EXAFS/CAS+S	0.34	-4.20	0.41	-2.00	-0.20	-0.12	0.005	-5.65	-0.12	-6.38	-0.39
EXAFS/DDCI2	0.33	-4.25	0.03	-2.03	-0.20	-0.08	0.0050	-6.13	-0.08	-6.40	-0.34
EXAFS/DDCI3	-1.11	-9.31	0.27	-3.76	-0.32	0.43	0.01	-14.24	0.44	-16.73	0.23

References

[1] Walter, M. D.; Booth, C. H.; Lukens, W. W.; Andersen, R. A. Cerocene revisited: the electronic structure of and interconversion between $Ce_2(C_8H_8)_3$ and $Ce(C_8H_8)_2$. *Organometallics* **2009**, *28*, 698.

[2] Warren, K. D. Ligand field theory of metal sandwich complexes. Magnetic properties of f^x configurations. *Inorg. Chem.* **1975**, *14*, 3095.

[3] Gourier, D.; Caurant, D.; Arliguie, T.; Ephritikhine, M. EPR and angle-selected ENDOR study of 5f-ligand interactions in the $[U(\eta^7\text{-}C_7H_7)_2]^-$ anion, an f^1 analogue of uranocene. *J. Am. Chem. Soc.* **1998**, *120*, 6084.

[4] Notter, F. P.; Bolvin, H. Optical and magnetic properties of the $5f^1$ AnX_6^{q-} series: a theoretical study. *J. Chem. Phys.* **2009**, *130*, 184310.

[5] Bolvin, H. An alternative approach to the g-matrix: theory and applications. *ChemPhysChem* **2006**, *7*, 1575.

[6] Abragam, A.; Bleaney, B. *Electronic paramagnetic resonance of transition ions;* Clarendon Press: Oxford, 1970.

[7] Chibotaru, L.; Ceulemans, A.; Bolvin, H. The unique definition of the g tensor of a Kramers doublet. *Phys. Rev. Lett.* **2008**, *101*, 033003.

[8] Bolvin, H.; Autschbach, J. Handbook of relativistic quantum chemistry. In ; Liu, W., Ed.; Springer: Berlin, 2017; Chapter Relativistic methods for calculating Electron Paramagnetic Resonance (EPR) parameters.

[9] Solis-Cespedes, E.; Páez Hernàndez, D. Modeling the electronic states and magnetic properties derived from the f1 configuration in lanthanocene and actinocene compounds. *Dalton Trans.* **2017**, *46*, 4834–4843.

[10] Gendron, F.; Páez Hernàndez, D.; Notter, F. P.; Pritchard, B.; Bolvin, H.; Autschbach, J. Magnetic properties and electronic structure of neptunyl(VI) complexes: Wavefunctions, orbitals, and crystal-field models.. *Chem. Eur. J.* **2014**, *20*, 7994.

[11] Páez Hernàndez, D.; Bolvin, H. Magnetic properties of a fourfold degenerate state: Np^{4+} ion diluted in Cs_2ZrCl_6 crystal. *J. Electron. Spectrosc. Relat. Phenom.* **2014**, *194*, 74.

[12] Kahn, O. *Molecular magnetism;* Wiley-VCH: New-York, 1993.

[13] Rota, J. B.; Knecht, S.; Fleig, T.; Ganyushin, D.; Saue, T.; Neese, F.; Bolvin, H. Zero-field splitting of the chalcogen diatomics using relativisitic correlated wave-function methods. *J. Chem. Phys.* **2011**, 114106.

[14] Anderson, P. W. Theory of magnetic exchange interactions: exchange in insulators and semiconductors. *Solid State Physics* **1963**, *14*, 99 – 214.

[15] Bloch, B. Sur la théorie des perturbations des états liés. *Nucl. Phys.* **1958**, *6*, 329–347.

[16] Calzado, C. J.; Cabrero, J.; Malrieu, J. P.; Caballol, R. Analysis of the magnetic coupling in binuclear complexes. II. Derivation of valence effective Hamiltonians from ab initio CI and DFT calculations. *J. Chem. Phys.* **2002**, *116*, 3985–4000.

[17] Bolvin, H. From ab initio calculations to model Hamiltonians: the effective Hamiltonian technique as an efficient tool to describe mixed-valence molecules.. *J. Phys. Chem. A* **2003**, *107*, 5071.